FROM INTERMOLECULAR INTERACTIONS TO INCIPIENT CHEMICAL BOND

Grzegorz CHALASINSKI[a], Jacek KLOS[a], Slawomir M. CYBULSKI
and Malgorzata M. SZCZESNIAK[c]

[a] *Department of Chemistry, University of Warsaw, Pasteura 1, 02-093 Warszawa, Poland*
[b] *Department of Chemistry, Miami University, Oxford, Ohio 45056, U.S.A.*
[c] *Department of Chemistry, Oakland University, Rochester, MI 48309, U.S.A.*

Received July 15, 1998
Accepted July 16, 1998

Dedicated to Professor Rudolf Zahradnik on the occasion of his 70th birthday.

The complexes of a rare gas atom (RG) and a number of open-shell molecules are discussed in the context of the bond character, structural and dynamical properties. The potential energy surfaces of a variety of complexes have been obtained using the combination of highly correlated supermolecular approach and the symmetry-adapted perturbation theory. Complexes of Σ-state species, O_2 and NH, display typical non-covalent interactions, similar to closed-shell systems. Complexes of Π-state species are represented by pairs of adiabatic potentials A′ and A″ due to removal of degeneracy through the interaction with the RG moiety. The two states may have distinctly different character. The He–CH($X^2\Pi$) complex displays an incipient π-bond on its A″ surface, while a regular van der Waals interaction is observed on the A′ surface. Interaction of a P-state chlorine atom with RG gives rise to two potential curves: Σ and Π. The Σ state features an incipient σ bond whereas the Π-state surface reveals a van der Waals interaction. The excited state complex He + $Cl_2(B^3\Pi_u)$ illustrates a different situation, with both the A′ and A″ states fairly close to each other, with only slight indication of the incipient bond.

Key words: Intermolecular interactions; van der Waals complexes; Molecular clusters; Rare gases complexes; *Ab initio* calculations.

An understanding of reactive interactions at the fundamental level has been one of the central goals of physical chemistry. As has been recognized since the early days of transition state theory, the shape of the potential energy surface (PES) dictates the reaction rate and the processes of energy disposal in the products. Today's reaction dynamics makes the connection between the overall shape and the particular features of the PES, such as barriers or local wells, and a success or failure of reactive events[1]. The understanding of this relationship allows us not only to predict the probability of reactive events, but also opens up a possibility of influencing the course of reactions by selectively modifying certain regions of PES (ref.[2]). One way to achieve a control of the reaction outcome is by orienting molecules and their orbitals as they approach one another[3]. Such attempts give rise to the emerging field of stereodynamics[4]. Another way of achieving prealigned systems is *via* the formation of a van der Waals system[5]. In these exciting developments the interactions involving open-shell radicals or excited state species are invaluable model systems.

A modeling of PESs of reactive interactions from the first principles is a very challenging proposition. Such a modeling must include the long-range part, which in the opinion of some[5] represents "one of the hardest regions to study, both experimentally and theoretically". Furthermore, it should be able to cope with the areas of incipient chemical bonding, where our understanding is incomplete at best. Finally, it must include the transition-state region where the expertise in all the types of interactions: covalent, non-covalent, and intermediate between them, is required.

Recent advances in crossed beam techniques coupled with spectroscopic methods have allowed for the monitoring of the reaction dynamics at a completely state-resolved level of detail[6,7]. High resolution supersonic jet spectroscopic techniques have been successfully employed to probe weakly bound molecules trapped in the wells due to the van der Waals or hydrogen-bond interactions[8]. The measurements of photofragment angular distributions resulting from the state-specific excitation have allowed the determination of dissociation energies in hydrogen-bonded complexes, such as $(HF)_2$ and its deuterated analogs[9]. State-to-state studies of laser excited vibrational transitions in prereactive molecular beams show that vibration excitation is sufficient to send reactants over the reaction barrier[10].

The open-shell species play a particularly important role in these studies because they open reactive channels on the PES making them much more complex. The long-range forces which operate in the entrance and exit channels can significantly affect the outcomes of chemical reactions. For example, orienting the reactants as they approach one another can increase the probability of reactive collisions. Conversely, if an entrance channel contained an attractive well before the barrier, the formation of long-lived collision complexes could lower the reaction probability. The elucidation of the effect the open- *versus* closed-shell species have in the interaction potential, and consequently, on the reaction dynamics is, thus, of fundamental importance.

The interactions involving open-shell species are, in principle, more anisotropic than closed-shell interactions. The presence of unpaired electrons may induce a new type of electronic anisotropy which is absent in the closed-shell case. For example, the interactions between two closed-shell atoms are fully angle-independent (isotropic), whereas the interactions between closed-shell and P-state atoms display angular dependence in many ways similar to that which is present in molecules. This electronic anisotropy plays a fundamental role in determining the strength and directionality of intermolecular forces, and leads to their description in terms of a manifold of potential energy surfaces[11].

Generally, PESs can either be extracted from the spectroscopic measurements *via* the so-called inversion procedures or calculated from first principles (*ab initio*) by solving an approximate electronic Schrödinger equation. However, in the case of open-shell interactions the inversion is very difficult because the spectroscopy does not sample a single PES, and it may be further complicated by the presence of the spin–orbit coupling and a possible breakdown of the Born–Oppenheimer approximation[12]. In such circumstances, the *ab initio* approaches for the calculations of PESs for open-shell interactions represent an invaluable resource, especially if such approaches are as successful as those proven reliable in calculations of closed-shell PESs (ref.[13]). One approach which results from the generalization of the closed-shell case to the unrestricted Hartree–Fock regime is particularly useful because it can dissect the surface into physically interpretable interaction energy terms: electrostatic, exchange, induction, and dispersion[14]. This technique combines the supermolecular unrestricted Møller–Plesset perturbation theory (UMPPT) or unrestricted coupled cluster theory (UCCSD(T)) with the symmetry-adapted perturbation theory (SAPT). The computational strategy which involves extended basis sets augmented with bond functions have been shown to generate PESs for these systems which are very reliable[15,16]. The decomposition of the surface into the physically interpretable terms is invaluable in analytical formulations of PESs. In this paper we summarize the results which have recently been obtained by using this approach for the complexes involving a rare gas atom interacting with the following open-shell species: $O_2(X^3\Sigma_g^-)$, $NH(X^3\Sigma^-)$, $CH(X^2\Pi)$, $Cl(^3P)$, and the excited triplet-state $Cl_2(B^3\Pi_u)$. In this series it is possible to observe a remarkable transition in the character of the interaction, from a typical long-range to the incipient chemical bond.

Rudolf Zahradník was one of the first who recognized this unified view of reactivity that encompasses both chemical and van der Waals reactivity[17]. He was far ahead of his time when he advocated the *ab initio* approach to these problems, even though in the 1960s and 1970s it looked as if these methods will never achieve the level of full predictability. Today, when the goal of predictability is near and we witness an astonishing progress in *ab initio* technology, it is necessary to give the due credit to Rudolf Zahradník's foresight and championship of *ab initio* approach.

STRATEGY OF *ab initio* CALCULATIONS OF ADIABATIC POTENTIALS

The calculations of the adiabatic potentials were performed by the supermolecular method. This approach derives the interaction energy as the difference between the energies of the dimer and the monomers:

$$\Delta E^{(n)} = E^{(n)}_{AB} - E^{(n)}_{A} - E^{(n)}_{B} \quad . \tag{1}$$

The superscript (n) denotes the level of theory, such as UHF, MPn, CCSD, *etc*. All the terms in Eq. (*1*) are evaluated within the same (dimer) basis set. This approach is equivalent to the counterpoise method of Boys and Bernardi[13,18,19].

The ΔE^{UHF} and $\Delta E^{(2)}$ (second-order Moller–Plesset correction) terms are interpreted in the framework of Intermolecular Moller–Plesset Perturbation Theory (I-MPPT). This encompasses well defined terms with clear physical meaning, such as electrostatics, exchange, induction, and dispersion. More information about connection between supermolecular and I-MPPT terms in the open-shell case can be found in the quoted papers[13,14].

CASE EXAMPLES

Ar–$O_2(X^3\Sigma_g^-)$: Interaction with Open-Shell Molecule

Ar(^{1}S)–$O_2(X^3\Sigma_g^-)$, was the first radical–RG complex to be observed spectroscopically. In 1973 Henderson and Ewing reported the Ar–O_2 infrared spectrum, proposed a model potential, and concluded that the complex has a T-shaped equilibrium geometry[20]. The models for RG–O_2 spectra calculations with explicit details of electronic and rotational angular momentum coupling have been available for some time[21]. Previous PESs developed by Gianturco and Strozhev[22] described reliably the Ar–O_2 interaction in the region of the global minimum, but were less accurate in the areas far from this region.

The state-of-the-art PES for Ar(^{1}S)–$O_2(X^3\Sigma_g^-)$, has recently been evaluated by Cybulski *et al.*[16]. This PES is shown in Fig. 1. The global minimum occurs for the T-shaped geometry, around 6.7 a_0. Our UMP4 estimate of the well depth of the global minimum is $D_e = 117\ \mathrm{cm}^{-1}$ and the related ground state dissociation energy obtained by diffusion

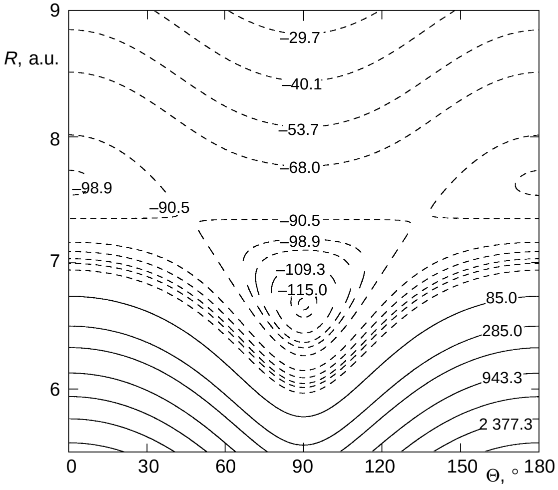

FIG. 1
Contour plot of the Ar(^{1}S)–$O_2(X^3\Sigma)$ potential

Monte-Carlo calculations is 96 cm^{-1}. These values are expected to be accurate to within a few per cent. The potential energy surface also reveals a local minimum for the collinear geometry at *ca* 7.6 a_0. The well depth for the secondary minimum at the UMP4 level is estimated at $D_e = 104$ cm^{-1}. The minima are separated by a barrier of 23 cm^{-1}. The global minimum is determined by the minimum in the exchange repulsion in the direction perpendicular to the O–O bond. The electron distribution of the ground state $O_2(X^3\Sigma_g^-)$, may be visualized as a dumbbell with a slight flattening at the ends. This is in agreement with the analysis of contour maps of the diffuse region of the Laplacian of the electron density of Bader[23]. A secondary, linear minimum is enhanced by a slight flattening of the electron density near the ends of the interoxygen axis.

Our parameters of the global minimum may be compared with previous empirical estimates. A good agreement is found with the most recent M3SVB1 surface, which is the best of the surfaces of Gianturco and Strozhev[22]. For M3SVB1 D_e amounts to 114.8 cm^{-1} at $R_e = 6.76$ a_0. The value of D_e falls within the ±5% error bar of our best result. A large discrepancy is found for the collinear form, which is expected since the experiment does not probe this region well. The interaction energy for the collinear geometry at $R = 7.0$ a_0 of *ca* –69.8 cm^{-1}, which is more than 21.9 cm^{-1} above *ab initio* values. In addition, the empirical potential has no barrier between the linear and T-shaped forms. Interestingly, the above result of –69.8 cm^{-1} is in good agreement with the interaction energy at the barrier of the *ab initio* potentials. This is reasonable if we assume that the anisotropy of M3SVB1 may be determined by the barrier for angular rotation. In fact, the anisotropy of M3SVB1 is superior to other empirical potentials.

Additional insight is provided by the dynamics of the system. From the contour of the ground rovibrational state (Fig. 2) it is clear that Ar performs a largely localized motion around the T-shaped from.

Finally, it is instructive to compare an open-shell $Ar–O_2(X^3\Sigma_g^-)$, with another Σ-symmetry complex: a closed shell $Ar–N_2(X^1\Sigma_g^-)$. In fact both complexes are fairly similar. For example, they possess global minima for the T-shaped form, their binding energies

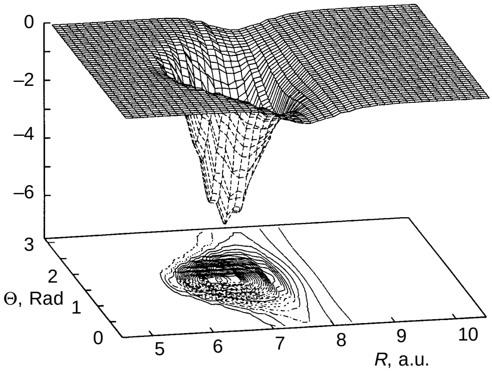

FIG. 2
The ground state Σ_0 rovibrational wavefunction for the $Ar(^1S)–O_2(X^3\Sigma_g^-)$ complex

fall in the same range (105–120 cm^{-1}), and so do the equilibrium distances[24] (6.9–7.0 a_0). An important difference, however, is the lack of a collinear local minimum in Ar–N_2. Another example of the Σ closed-shell complex which is similar to Ar–$O_2(X^3\Sigma_g^-)$ is CO–Ar. CO–Ar is essentially T-shaped (with Ar slightly shifted towards O) with D_e = 110 cm^{-1} and R_e = 7 a_0 (ref.[25]). Overall, Ar–$O_2(X^3\Sigma_g^-)$, resembles a closed-shell species, and shows no evidence of any incipient chemical bonding.

Ar–NH($X^3\Sigma^-$): Interaction with Radical

Over the last several years, we have witnessed a concerted experimental and theoretical effort to characterize a variety of RG–hydride radical systems in states of different space and spin symmetries[26,27]. One of the simplest first-row atom radicals is the NH diatomic. The van der Waals complexes of Ar and the NH radical in the first three states, $X^3\Sigma^-$, $a^1\Delta$, and $b^1\Sigma^+$, were studied *ab initio* by Jansen and Hess[28]. Very recently, the next state, a singlet $c^1\Pi$, has been thoroughly examined in a combined *ab initio* and experimental study of Yang *et al.*[29]. However, due to demanding nature of these type of calculations[13] the resulting PESs were too shallow and have to be appropriately modified for the simulations of spectroscopic and scattering experiments[30–32].

Recently, the state-of-the-art PES was advanced for the Ar(^{1}S) + NH($X^3\Sigma^-$) interaction by our group[15]. The $X^3\Sigma^-$ is the lowest triplet state of the Σ symmetry, which originates from the $K(2s\sigma)^2(2p\sigma)^2(2p\pi)^2$ configuration. The global minimum occurs for the approximate T-shaped geometry with Ar skewed towards the H atom at about Θ = 67° and R = 6.75 a_0. Our UMP4 estimate of the well depth of the global minimum is D_e = 100.3 cm^{-1} and the related ground state dissociation energy obtained by rigid-body diffusion quantum Monte-Carlo calculations (RBDQMC) and by the collocation method is D_0 = 71.5 cm^{-1}. These values are expected to be accurate to within a few per cent. The potential energy surface also features a wide plateau in the proximity of Ar–N–H collinear geometry, at *ca* 7.0 a_0. Overall, the PES is remarkably flat. The energy difference between the lowest point on the surface and the plateau is only 10–13 cm^{-1}. Furthermore, beginning with R = 7 a_0 the PES exhibits wide areas with energy nearly independent of Θ; the PES is, thus, fairly isotropic. The RBDQMC and collocation calculations reveal nearly a free rotation of the NH subunit in the complex. This is seen in Fig. 3 where the ground rovibrational state wavefunction is displayed.

Decomposition of the interaction energy provides insights into the nature of bonding and the sources of anisotropy. The global equilibrium point, if compared to the collinear arrangements, features enhanced dispersion attraction and reduced exchange repulsion. The enhanced dispersion is obviously related to the closer approach of Ar toward the nitrogen atom. Closer approach is usually accompanied by the increase of the exchange effect[13]. Interestingly, in the Ar–NH complex the situation is different, and on approaching N the exchange repulsion undergoes reduction. This may be attributed to the depletion of the electron charge density in this region. Interestingly, the induction energy, often an important structural factor, is relatively small and not very anisotropic (in contrast to Ar–HF or Ar–HCl).

He–CH(X $^2\Pi$): Incipient π Bond

The $X^2\Pi$ state of CH corresponds to the $1\sigma^2 2\sigma^2 3\sigma^2 1\pi^1$ configuration, and gives rise to two electronic states[33] of the CH–He complex, $^2A'$ and $^2A''$. These states are related to two different orientations of He with respect to the singly occupied 1π orbital of CH: $^2A'$ corresponds to 1π located in the C–H–He plane, and $^2A''$ corresponds to 1π perpendicular to the C–H–He plane.

It has been found that the two states are distinctly different[34]. The A′ state's PES represents a typical van der Waals interaction which is characterized by two similarly deep minima. The first minimum occurs for the collinear He–C–H arrangement, at R ≈ 7.5 a_0, and Θ = 0°, and is 12.1 cm^{-1} deep. The second minimum has a trough-like form which joins the region between $R = 7.5\ a_0$, $\Theta = 140°$ and $R = 8.0\ a_0$, $\Theta = 180°$. The lowest point is approximately 11.9 cm^{-1} deep and occurs at $R = 7.5\ a_0$ and $\Theta = 140°$. The shape and location of these minima is determined primarily by the anisotropy of the dispersion component.

In contrast, the potential energy surface (PES) of the A″ state has only a single and relatively deep minimum of $D_e \approx 73.5\ cm^{-1}$ for the T-shaped geometry, at $R = 5.0\ a_0$ and $\Theta = 100°$. The position of this minimum is determined by the exchange repulsion, which is substantially reduced at this geometry. The minimum is unusually deep for a complex of He.

Why do we observe such a significant difference between the A′ and A″ states? This may be rationalized as follows: For the π^1 configuration, a rare-gas atom faces either coplanar singly filled π orbital (A′) or a σ orbital. Facing an electron in π orbital leads to a considerable rise of repulsion in comparison to facing an electron in σ orbital because of the nodal plane and different symmetries. Thus, in the latter case the ex-

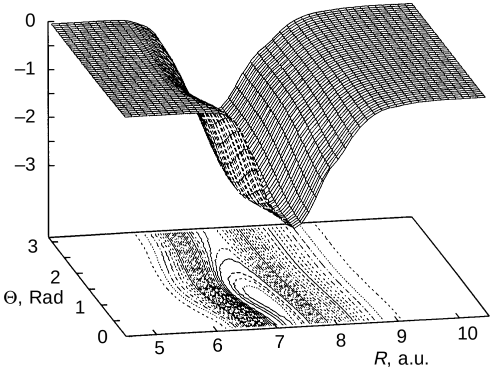

FIG. 3
The ground state Σ_0 rovibrational wavefunction for the $Ar(^1S)–NH(X^3\Sigma^-)$ complex

change repulsion is significantly diminished, and allows He for closer approach and larger binding.

It is instructive to analyze in more detail the location and depth of the global minima. The deep minimum for the A″ state does not occur at the H-bonded geometry, but for the T-shaped structure. To better appreciate how unusually low it is, we may compare it to the minimum for a relatively strong complex of He, He–HF (D_e = 39.3 cm^{-1}). In the latter case the H-bond structure is actually forced by the induction effects since the exchange niche occurs for the T-shaped configuration. The dipole moment of CH is somewhat smaller than that of HF (1.65 *versus* 1.82 a.u.) and it does not seem to have anything to do with the stabilization of the A″ state, as the complex is T-shaped. The driving force is a considerable reduction of the exchange effects for the T-shaped form. Whereas the reduction of repulsion for the T-shaped configuration has been observed for many van der Waals species (RG–CO, ref.[25]; RG–Cl_2, ref.[35]; RG–O_2, refs[16,36]; *etc*.) in this particular case it is unusually large. It is best demonstrated in Fig. 4 where we plotted the ratio of $\varepsilon^{(20)}_{\text{disp}}/\varepsilon^{\text{HL}}_{\text{exch}}$ and $\Delta E^{\text{UHF}}_{\text{def}}/\varepsilon^{\text{HL}}_{\text{exch}}$. The first of these ratios reveals unexpected dip around 100°. It is clear that something happens there which has to do with the sudden drop in the HL-exchange repulsion contributes to the strong binding of He and CH in this state. One may view this effect as the incipient chemical bond. Since it conserves the π nodal plane it may be dubbed an “incipient π bond”.

Another example of such an “incipient π bond” has been recently reported for the He(^{1}S)–Li(^{2}P) complex by Bililign *et al.*[37]. An anomalously reduced repulsion in interaction of the $1s^2$ configuration with a Π state in the π nodal plane was found and nicely rationalized. They pointed out that in this case the HL-exchange repulsion is reduced due to symmetry and consequently there is no repulsive contribution which would engage the s-symmetry He orbital and the p-symmetry Li orbital perpendicular to the He–Li axis. Yet dispersion interaction between the same orbitals takes place as usual, and there is no similar reduction of attraction.

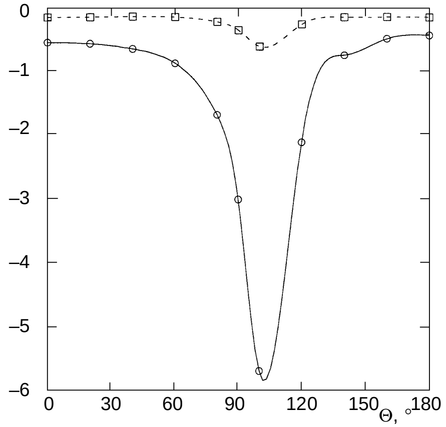

FIG. 4

Angular dependence of the ratios: UHF-deformation against HL-exchange, and dispersion against HL-exchange energies for the ^{2}A″ state of He–CH($X^2\Pi$) at R = 6.5 a_0; ❐ and dashed line, $\Delta E^{\text{SCF}}_{\text{del}} : \varepsilon^{\text{HL}}_{\text{exch}}$; ❍ and solid line, $\varepsilon^{(20)}_{\text{disp}} : \varepsilon^{\text{HL}}_{\text{exch}}$

RG–Cl(^3P): Incipient σ Bond

The state-of-the-art *ab initio* potential curves for the lowest adiabatic states $X^2\Sigma$ and $A^2\Pi$ of three RG–Cl (RG = He, Ne, Ar) complexes have been recently calculated[38]. The Σ states are almost twice as deep as the Π states, and their minima occur at significantly shorter interatomic distances. A comparison of the interaction in the Σ and Π states reveals a qualitatively different nature of the van der Waals bonding. The Σ complex may be thought of as a complex which differs from a regular closed-shell RG–RG dimer by a removal of a single electron along the interatomic axis. The RG–X repulsion is thus weakened and the interaction is strengthened accordingly. We may call this situation an incipient chemical bond of σ-symmetry. By way of contrast, the Π complex can be viewed as bound by a regular van der Waals bond, not much different from RG–RG, since the electron is removed from an orbital that is perpendicular to the interatomic axis. These conclusions are confirmed by the comparison of D_e and R_e of Ar–Cl with those of Ar–Ar. In the Π state Ar–Cl D_e amounts to 88.9 cm^{-1}, which is indeed close to 99.6 cm^{-1} of Ar–Ar (ref.[39]). R_e is somewhat longer than that of Ar–Ar (by 0.38 a_0). The Σ state of Ar–Cl is almost twice as deep as Ar–Ar, with R_e shorter by almost 0.57 a_0. In the same spirit, the He–Ar interaction may be viewed as a prototype of the Π state of He–Cl. Indeed, D_e of He–Ar amounts to 20.4 cm^{-1} (ref.[40]), to be compared with 15.1 cm^{-1} for He–Cl. The Σ state of He–Cl has the well depth of 29.0 cm^{-1}. It should be stressed that the difference between the "one-electron" and "two-electron" van der Waals contact resides almost entirely in the exchange repulsion term, with the dispersion term varying little in these two states.

He–Cl_2($B^3\Pi_u$): Interaction in an Excited State

RG–halogen molecule complexes have served as the favorite model systems in the studies of the effect of interactions upon the dynamics of energy redistribution ever since Valentini and Cross[41] demonstrated the dramatic effect of the interaction with the rare gas atom upon the photodissociation of I_2 in the so-called one atom cage effect. The state-to-state excitation spectra from the X state to the selected vibrational levels of the B state of He–Cl_2 have been measured in pump-probe experiments by Janda *et al.*[42]. Simulations of such experiments require detailed knowledge of the potential energy surfaces of both the X and the B state. The calculations of Chalasinski *et al.*[35] determined the nature of PES for the X state. The PES contains two minima – the deeper one for the L-configuration and the shallower one for the T-shaped configuration. As shown by Huang *et al.*[43] the ground vibrational state is located in the shallower minimum due to the zero-point effect. The first triplet state results from promoting an electron from a $(\pi^*)^4$ to a $(\pi^*)^3\sigma^*$ configuration[14,44]. This configuration leads to a 3P state which in the presence of RG approaching from any direction except collinear causes a split into two states $^3A'$ and $^3A''$. In the A'' state the π*-orbital facing He is doubly occupied and hence this is quasi-closed-shell state. The PES in this state indeed resembles that of the ground state since it contains two minima; one for the T- and the second, much shallower, for the L-configuration. The well depth calculated at the CCSD(T) level of theory for this state was 318 cm^{-1} at $R = 6.73\ a_0$. With the A′ state in which He faces the singly occupied π* orbital, the surface topography is different, involving only a single, shallower minimum for the T-configuration of 25.6 cm^{-1} at $R = 6.97\ a_0$. The origin of this difference lies again in the different behavior of the exchange repulsion in two states. When He moves around Cl_2 starting from the L structure it first experiences less repulsion within the A′ state than in the A″ state consistently with a simple intuition that the singly occupied π* orbital would repel He less strongly than the doubly occupied. However, in the proximity of the T-configuration, *i.e.* close to the π* orbital nodal plane perpendicular to the Cl–Cl bond, the order of repulsion suddenly reverses. For example at $\Theta = 90°$ and $R = 7.1\ a_0$ the exchange repulsion in the A′ state is larger by a factor of 2.5 than in the A″ state. The smaller repulsion in the A″ state allows for a closer approach of monomers and the attractive dispersion interaction to take over. As shown in Fig. 5, there is analogous (but not as dramatic) enhancement of dispersion attraction in the A″ state as in He–CH (see Fig. 4). However, to say that these differences can be rationalized at this level of theory would be deceptive. Our calculations show that the quantitative balance of both states' well-depths can only be achieved upon inclusion of the high order correlation effects in the CCSD(T) approach. For example, at the MP4(SDTQ) level of theory the A′ state is only slightly less stable than A″ (by *ca* 1.3 cm^{-1}). The inclusion of the coupled cluster excitations brings the energy gap to *ca* 6.6 cm^{-1} by dramatically reducing the well-depth of the A′ state and a slight deepening the A″ state. The dramatic influence of the iterative single excitations on the A′ state is worth noting.

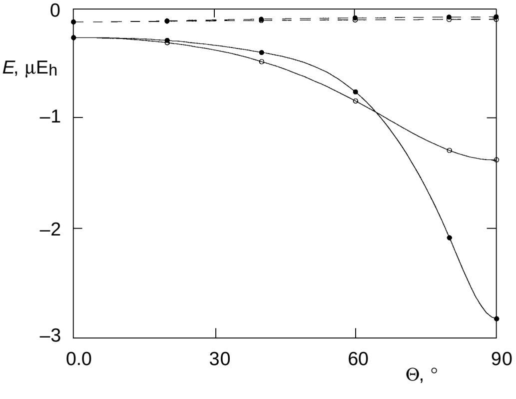

FIG. 5
Angular dependence of the ratio: UHF-deformation against HL-exchange (solid lines), and dispersion against HL-exchange energies (dashed lines) for two states: $^2A'$ (open circles) and $^2A''$ (filled circles) of He–$Cl_2(B^3\Pi_u)$ at $R = 7.1\ a_0$

SUMMARY

Complexes of rare gas atoms with open-shell species allow us to probe binding which is intermediate between a van der Waals attraction and a covalent bond. It has been shown that both σ-type and π-type contact between a singly occupied orbital and a closed shell may lead to unusual enhancement of the interaction energy, which exceeds a regular van der Waals bond strength.

The Σ state Cl–RG complex was shown to feature an incipient σ-bond, and the A″ state of He–CH($X^2\Pi$) provided an example of an incipient π-bond. We also found that the increase of binding energy is always due to reduction of the exchange repulsion, whereas the attraction, primarily dispersion, is less sensitive. Finally, we have shown examples where the difference between the singly- and doubly-occupied orbital contacts with a closed shell is small, and is overwhelmed by higher-order correlation effects (He–Cl_2($B^3\Pi_u$)).

The authors (M. M. S. and G. C.) thank the National Science Foundation, grant No. CHE-9527099, and one of us (S. M. C.) thanks the National Science Foundation, grant No. CHE-9616683.

REFERENCES

1. Bernstein E. R. (Ed.): *Chemical Reactions in Clusters*. Oxford University Press, Oxford 1996.
2. Jouvet C., Solgadi D. in: Ref.[1], p. 100.
3. Pullman D. B., Friedrich B., Herschbach D. R.: *J. Chem. Phys*. **1990**, *93*, 3224.
4. *J. Phys. Chem. A* **1997**, *101*, Issue No. 41.
5. Meijer A. J. H. M., Groenenboom G. C., van der Avoird A.: *J. Phys. Chem*. **1997**, *101*, 7558.
6. Wittig C., Zewail A. H. in: Ref.[1], p. 64.
7. Valentini J. J.: *Faraday Discuss. Chem. Soc*. **1991**, *91*, 392.
8. a) Nesbitt D. J., Nibler J. W., Schiffman A., Chapman W. B., Hutson J. M.: *J. Chem. Phys*. **1993**, *98*, 9513; b) Saykally R. J.: *Acc. Chem. Res*. **1989**, *22*, 295.
9. Bohac E. J., Marshall M. D., Miller R. E.: *J. Chem. Phys*. **1992**, *96*, 6681.
10. Anderson D. T., Schwartz R. L., Todd A., Lester M. I.: *J. Chem. Phys*. **1998**, *109*, in press.
11. Aquilanti V., Liuti G., Pirani F., Vecchiocattivi F.: *J. Chem. Soc., Faraday Trans*. **1989**, *2*, 85.
12. Dubernet M.-L., Flower D., Hutson J. M.: *J. Chem. Phys*. **1991**, *94*, 7602.
13. Chalasinski G., Szczesniak M. M.: *Chem. Rev*. **1994**, *94*, 1724.
14. Cybulski S. M., Burcl R., Chalasinski G., Szczesniak M. M.: *J. Chem. Phys*. **1995**, *103*, 10116.
15. Kendall R. A., Chalasinski G., Klos J., Bukowski R., Severson M. W., Szczesniak M. M., Cybulski S. M.: *J. Chem. Phys*. **1998**, *108*, 3235.
16. Cybulski S. M., Kendall R. A., Chalasinski G., Severson M. W., Szczesniak M. M.: *J. Chem. Phys*. **1997**, *106*, 7731.
17. Hobza P., Zahradnik R.: *Weak Intermolecular Interactions in Chemistry and Biology*. Academia, Prague 1980; Elsevier, Amsterdam 1980.
18. Boys S. F., Bernardi F.: *Mol. Phys*. **1970**, *19*, 553.
19. a) van Lenthe J. H., van Duijneveldt-van de Rijdt J. G. C. M., van Duijneveldt F. B.: *Adv. Chem. Phys*. **1987**, *69*, 521; b) Gutowski M., Szczecniak M. M., Chalasinski G.: *Chem. Phys. Lett.* **1995**, *241*, 140.

20. Henderson G., Ewing G. E.: *J. Chem. Phys*. **1973**, *59*, 2280.
21. a) Tennyson J., Mettes J.: *Chem. Phys*. **1983**, *76*, 195; b) van der Avoird A.: *J. Chem. Phys*. **1983**, *79*, 1170; c) Tennyson J., van der Avoird A.: *Chem. Phys. Lett.* **1984**, *105*, 49.
22. Gianturco F. A., Storozhev A.: *J. Chem. Phys*. **1994**, *101*, 9624.
23. Bader R. F. W.: *Atoms in Molecules – A Quantum Theory*. Oxford University, Oxford 1990.
24. Wang F., McCourt F. R. W., Le Roy R. J.: *Mol. Phys*. **1996**, *88*, 821.
25. Kukawska-Tarnawska B., Chalasinski G., Olszewski K.: *J. Chem. Phys*. **1994**, *101*, 4964.
26. Heaven M. C.: *Annu. Rev. Phys. Chem*. **1992**, *43*, 283.
27. Heaven M. C.: *J. Phys. Chem*. **1993**, *97*, 8567.
28. Jansen G., Hess B. A.: *Chem. Phys. Lett*. **1992**, *192*, 21.
29. Yang M., Alexander M. H., Werner H.-J., Hohmann J., Neitsch L., Stuhl F., Dagdigian P. J.: *J. Chem. Phys*. **1995**, *102*, 4069.
30. Schmelz T., Rosmus P., Alexander M. H.: *J. Phys. Chem*. **1994**, *98*, 1073.
31. Alexander M. H., Gregurick S., Dagdigian P. J.: *J. Chem. Phys*. **1994**, *101*, 2887.
32. Alexander M. H., Gregurick S., Dagdigian P. J., Lemire G. W., McQuaid M. J., Sausa R. C.: *J. Chem. Phys*. **1994**, *101*, 4547.
33. Wagner A. F., Dunning T. H., Jr., Kok R.: *J. Chem. Phys*. **1994**, *100*, 1326.
34. Cybulski S. M., Chalasinski G., Szczesniak M. M.: *J. Chem. Phys*. **1996**, *105*, 9525.
35. Chalasinski G., Gutowski M., Szczesniak M. M., Sadlej J., Scheiner S.: *J. Chem. Phys*. **1994**, *101*, 6800.
36. Cybulski S. M., Burcl R., Szczesniak M. M., Chalasinski G.: *J. Chem. Phys*. **1996**, *104*, 7977.
37. Bililign S., Gutowski M., Simons J., Breckenridge W. H.: *J. Chem. Phys*. **1994**, *100*, 8212.
38. Burcl R., Krems R. V., Buchachenko A. A., Szczesniak M. M., Chalasinski G., Cybulski S. M.: *J. Chem. Phys*., in press.
39. Aziz R. A.: *J. Chem. Phys*. **1993**, *99*, 4518.
40. Aziz R. A., Riley P. W., Buck U., Maneke G., Schleusener J., Scoles G., Valbusa U.: *J. Chem. Phys*. **1997**, *71*, 2637.
41. Valentini J. J., Cross J. B.: *J. Chem. Phys*. **1982**, *77*, 572.
42. Cline J. I., Evard D. D., Thommen F., Janda K.: *J. Chem. Phys*. **1986**, *84*, 1165.
43. Huang S. S., Bialer C. R., Tao F.-M., Klemperer W., Casavecchia P., Volpi G. G., Halberstadt N., Janda K.: *J. Chem. Phys*. **1995**, *102*, 8846.
44. Rohrbacher A., Williams J., Janda K., Cybulski S. M., Burcl R., Szczesniak M. M., Chalasinski G., Halberstadt N.: *J. Chem. Phys*. **1997**, *106*, 2685.